CMS Physics Analysis Summary

Contact: cms-pag-conveners-top@cern.ch 2015/12/15

Underlying event measurement with $t\bar{t}$ + X events with p-p collision data at $\sqrt{s}$ =13 TeV

The CMS Collaboration

Abstract

Measurements of the underlying event (UE) activity using charged particle properties in $t\bar{t}$ events in the μ + jets channel are presented. Proton-proton collision events at a center-of-mass energy of $\sqrt{s} = 13$ TeV, corresponding to an integrated luminosity of 2.2 fb^{-1} recorded by the CMS detector at the LHC, are used for the measurements. The measurements are found to be consistent with the predictions from the QCD Monte Carlo model generators used by CMS for the LHC Run II data.

1 Introduction

LHC Run-II measurements at ultimate precision require improved modeling and dedicated measurements of top quark events. One of the important ingredients in simulations is the description of the underlying event (UE). Over the last several years our understanding and modeling of the UE in a hard-scattering process has improved greatly. The UE consists of the beam-beam remnants and the multiple parton interactions that accompany the hard scattering. However, the observables used to study the UE also receive contributions from initial and final state radiation, making it difficult to uniquely identify the various components of the scattering. One uses the topological structure of hard hadron-hadron collisions to study the UE experimentally. As illustrated in Fig. 1, on an event-by-event basis, the direction of a "leading object" is used to define regions of η-ϕ space, where η is the pseudo-rapidity and ϕ is the azimuthal scattering angle. One then examines the number of charged particles and the scalar transverse momentum (p_T) sum of the charged particles in the "toward", "away", and "transverse" regions. The "transverse" region is very sensitive to the modeling of the UE.

At the LHC, the UE has been measured using minimum bias events [1–5], Drell-Yan events [6], and $t\bar{t}$ events [7]. These studies have used the highest transverse momentum charged particle, the highest transverse momentum charged-particle jet, the highest transverse energy calorimeter jet, and the lepton-pair in Z-boson production as the "leading object". In this analysis, using 13 TeV data, we study the UE in top-quark production and use the $t\bar{t}$ pair as the "leading object" as in the earlier CMS measurement at 8 TeV [7].

QCD Monte Carlo (MC) generators such as PYTHIA [8] and HERWIG ++ [9] have parameters that may be adjusted to control the behavior of their event modeling. A specified set of these parameters that has been adjusted to better fit some aspects of the data is referred to as a "tune". The PYTHIA 8 tune CUETP8M1 [10] and the HERWIG ++ tune EE5C [11] are constructed by fitting the UE data at several center-of-mass energies, where the "leading object" is the highest transverse momentum charged particle or the highest transverse momentum charged-particle jet in the event. These tunes also describe well the UE as measured in Z-boson production. However, very little is known about the UE in heavy quark production.

This note represents a "first look" in which we compare detector-level top-quark production data at 13 TeV with the PYTHIA 8 tune CUETP8M1 and the HERWIG ++ tune EE5C after detector simulation.

In Section 2, a description of the data and MC samples used in this measurement is given. In Section 3, the event reconstruction and selection are described and in Section 4 the measured variables are defined and the results are presented.

2 Data and Monte Carlo Samples

Proton-proton collision data at center of mass energy of 13 TeV and bunch crossing of 25 ns recorded by CMS experiment [12] are used in this analysis. The total integrated luminosity of the data used is 2.2 fb^{-1}.

The $t\bar{t}$ signal processes as well as the single-top quark backgrounds have been simulated on the basis of a Next-to-Leading Order (NLO) calculation using the POWHEG v2 generator [13–15]. The W+jets background is simulated with the MG5_aMC@NLO [16] generator. The assumed top quark mass in the simulations is 172.5 GeV. Parton showering and hadronization are simulated with PYTHIA 8 and as an alternative, with HERWIG ++. The underlying event tunes used in these simulations are CUETP8M1 and EE5C with PYTHIA 8 and HERWIG ++, respectively.

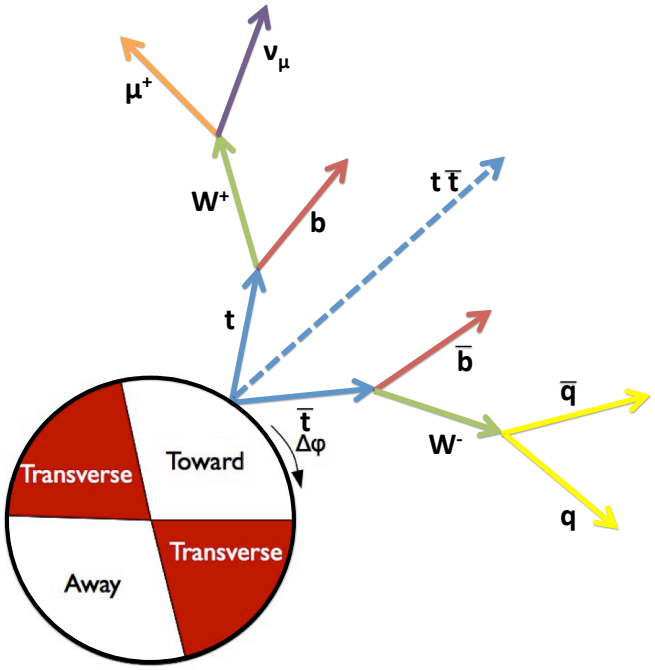

Figure 1: Schematic view of the UE regions defined with respect to the azimuthal angle difference between the charged particle candidate and the axis of the $t\bar{t}$ system with a schematic diagram of $t\bar{t}$ decay chain.

The factorization and renormalization scales are set to the transverse mass of the top quark m_T^t in the $t\bar{t}$ rest frame and the PDF set used is NNPDF3.0 [17]. The generated events are processed through the CMS detector simulation and reconstruction. The detector simulation is based on GEANT4 [18]. To compare the results with simulations assuming different scale choices, samples with scales varied in the parton shower calculations are used. The simulated samples are re-weighted to match the observed distribution of pile-up events.

3 Event Selection

The data were selected online by requiring the presence of a single muon with transverse momentum (p_T) above 20 GeV. Isolation and identification criteria are also applied at the trigger level.

The particle-flow (PF) event algorithm reconstructs and identifies each individual particle with an optimized combination of information from the various elements of the CMS detector. The energy of photons is directly obtained from the ECAL measurement. The energy of electrons is measured from a combination of the electron momentum at the primary interaction vertex as determined by the tracker, the energy of the corresponding ECAL cluster, and the energy sum of all bremsstrahlung photons spatially compatible with originating from the electron track. The energy of muons is obtained from the curvature of the corresponding track. The energy of charged hadrons is determined from a combination of their momentum measured in the tracker and the matching ECAL and HCAL energy deposits. Finally, the energy of neutral hadrons is obtained from the corresponding corrected ECAL and HCAL energies.

Muons are measured in the pseudo-rapidity range $|\eta| < 2.4$, with detection planes exploiting

three technologies: drift tubes, cathode strip chambers, and resistive plate chambers. Matching muons to tracks measured in the silicon tracker results in a relative transverse momentum resolution for muons with $20 < p_{\mathrm{T}} < 100\,\mathrm{GeV}$ of 1.3–2.0% in the barrel and better than 6% in the endcaps; the p_{T} resolution in the barrel is better than 10% for muons with p_{T} up to 1 TeV [19]. The muon candidates are required to have a transverse momentum $p_T > 22$ GeV and to be in the region $|\eta| < 2.4$. The track to the muon candidate is required to have more than a minimum number of silicon tracker hits, to have a high-quality tracker-muon system global fit with more than a minimum number of hits in the muon detectors, and to be consistent with the primary vertex. A PF-based relative isolation requirement is imposed on each muon candidate for which pileup effects are corrected. The scalar sum of the transverse momenta of the reconstructed PF candidates within a cone of size $R = \sqrt{\Delta\eta^2 + \Delta\phi^2} < 0.4$ around the direction of the muon is required to be less than $0.15 \times p_T^{\mu}$. For each event, exactly one muon satisfying all the above requirements is required to be present. The events with extra isolated muons with $p_T > 15$ GeV and $|\eta| < 2.4$ are discarded.

For each event, hadronic jets are clustered from the reconstructed particles with the infrared and collinear safe anti-k_{t} algorithm, with a size parameter R of 0.4. The jet momentum is determined as the vectorial sum of all particle momenta in the jet, and is found in the simulation to be within 5% to 10% of the true momentum over the whole p_{T} spectrum and detector acceptance. Jet energy corrections are derived from the simulation, and are confirmed with in situ measurements with the energy balance of dijet and photon+jet events [20].

At least four jets with $p_T > 30$ GeV and $|\eta| < 2.4$ are required to be present in each event. Jets that match the muon within $\Delta R < 0.4$ are removed. Among the selected jets, two of them are required to be identified as heavy flavor jets based on the Combined Secondary Vertex (CSV) [21] algorithm with a working point yielding 65% efficiency for b jets and 3% acceptance for light quark and gluon jets.

In the measurement, charged PF candidates with $p_T > 500$ MeV and $|\eta| < 2.1$ are selected if the following conditions are satisfied: longitudinal distance from the primary vertex <1 cm, its significance < 10, transverse distance to the primary vertex <3 cm, and its significance < 10 . In addition a tight primary vertex association is required. The PF constituents of the four jets identified with the $t\bar{t}$ decay are removed if they are within $\Delta R = 0.05$ of the jet constituents. Similarly, the muons that are within $\Delta R = 0.05$ from the PF candidates are removed.

The number of selected events in the data after the kinematic reconstruction, described in the next section, is 23125. The purity of the selected sample is expected to be 91%. The data and theory predictions for the total event yields agree well within the systematic uncertainties due to integrated luminosity, cross-section calculations, jet energy scale, and pile-up. In the analysis, the backgrounds are not subtracted; their effect is expected to be 1% in all the presented distributions.

4 Measurements

4.1 Kinematic Reconstruction

We reconstruct the kinematics of the $t\bar{t}$ system in the $\mu + jets$ final state. In each event, the leptonically decaying W boson is reconstructed using the lepton momentum and the transverse component of the missing energy measurements. The longitudinal component of the neutrino, $p_{Z,\nu}$, is determined by means of a quadratic equation, with the constraint that the reconstructed W boson mass be 80.4 GeV. This equation yields complex solutions for 34% of the events. For

Table 1: Definition of the soft event regions.

toward	$\Delta\phi < 60^\circ$
transverse	$60^\circ < \Delta\phi < 120^\circ$
away	$\Delta\phi > 120^\circ$

these events, the x and y components of the transverse missing momentum are varied to make the W boson transverse mass ($m_{T,W}$) equal to 80.4 GeV. As a result of this, 89% of the events with complex solutions are recovered. The jet pair that gives the invariant mass closest to 80.4 GeV is selected among the jets that are not b-tagged. This pair is assigned to the hadronic top quark (t_{had}). The two (or one) neutrino solutions are used to select the lepton-neutrino-b-jet combination that gives the invariant mass closest to the top quark mass of 172.5 GeV. This combination corresponds to the leptonic top quark (t_{lep}). The remaining b-tagged jet is assigned to the hadronic top quark.

The following azimuthal angle is defined to characterize soft events:

$$\phi^k = tan^{-1}\frac{p_y^k}{p_x^k}, \tag{1}$$

where k represents either the $t\bar{t}$ system or a charged particle candidate. The soft event regions are defined as in Table 1 using the azimuthal angle difference between the $t\bar{t}$ system and the charged particle candidates, $\Delta\phi$. The charged PF candidates found in a 60° around $\phi^{t\bar{t}}$ are considered to be produced in the "toward" direction, while the particles in the opposite direction are considered to be produced in the "away" direction. The charged particles remaining within $60 - 120^\circ$ of $\phi^{t\bar{t}}$ are considered to be produced in the "transverse" direction. The transverse and toward regions are expected to be mostly populated by the soft event activity, to be sensitive to the multi-parton-interactions and beam-beam-remnant components of the underlying event. The away region is sensitive to the modeling of the recoil of the $t\bar{t}$ system.

4.2 Categorization of the Events

To study the effect of the modeling of the recoil, the sample is studied inclusively, as well as in three jet multiplicity bins: 0, 1, and $\geq$2 jets. The jets are required to have $p_T > 15$ GeV and to be produced in association with the $t\bar{t}$ event. In this note, these jets are referred to as extra jets.

The measured quantities are the charged multiplicity (N_{ch}), the scalar sum of the transverse momenta of the charged particles (Σp_T), and the average transverse momentum per charged particle $\overline{p}_T$. The stability of the measurement with respect to pile-up is verified by measuring N_{ch} and Σp_T for different numbers of primary vertices.

The uncertainty originating from the modeling of the initial- and final-state-radiation (ISR/FSR) in $t\bar{t}$ events is expected to be accounted for by the factorization and renormalization scale uncertainties. These are calculated by using dedicated $t\bar{t}$ samples in which the renormalization scale in the parton shower simulation is varied by factors of 2 and 0.5.

4.3 Charged Particle Activity

In Figs. 2-4, the distributions of N_{ch}, Σp_T and $\overline{p}_T$ are shown for the overall sample and the three regions defined in the previous section. Distributions obtained with the nominal Q^2 scale as well as $(2Q)^2$, and $(Q/2)^2$ are displayed separately. The predictions from the POWHEG + PYTHIA

8 generator agree well with data in all regions, though a slightly better agreement is observed for charged multiplicities smaller than about 50. For charged particle multiplicities higher than ∼50, POWHEG + PYTHIA 8 predicts a higher multiplicity especially in the away region.

Distributions of average N_{ch}, Σp_T and $\overline{p}_T$ are displayed in Figs. 5-7 with respect to the azimuthal angle between the $t\bar{t}$ system and the charged PF candidate ($\Delta\phi$) and in Figs. 8-7 with respect to $p_T(t\bar{t})$. When there are no extra jets (i.e. no jets other than the four jets associated with the $t\bar{t}$ production) with $p_T(j) > 15$ GeV and $|\eta|$ <2.4, only a very small increase in N_{ch}, Σp_T or $\overline{p}_T$ with increasing $\Delta\phi$ is observed. Conversely, as the number of extra jets increases, N_{ch}, Σp_T and $\overline{p}_T$ grow significantly with $\Delta\phi$. This may be explained by the fact that in the presence of an extra jet in the event, more of the recoil particles are clustered in the jet and the $t\bar{t}$ system becomes more boosted. This is supported by Figs. 8-10, which show that N_{ch}, Σp_T and $\overline{p}_T$ increase with $p_T(t\bar{t})$ only in the away direction. In Figs. 5-10, data at the detector level are compared to POWHEG + PYTHIA 8 and POWHEG + HERWIG ++ predictions with different renormalization scales. The scale dependence is most prominent in the UE observables measured as a function of $p_T(t\bar{t})$ for events with no extra jets.

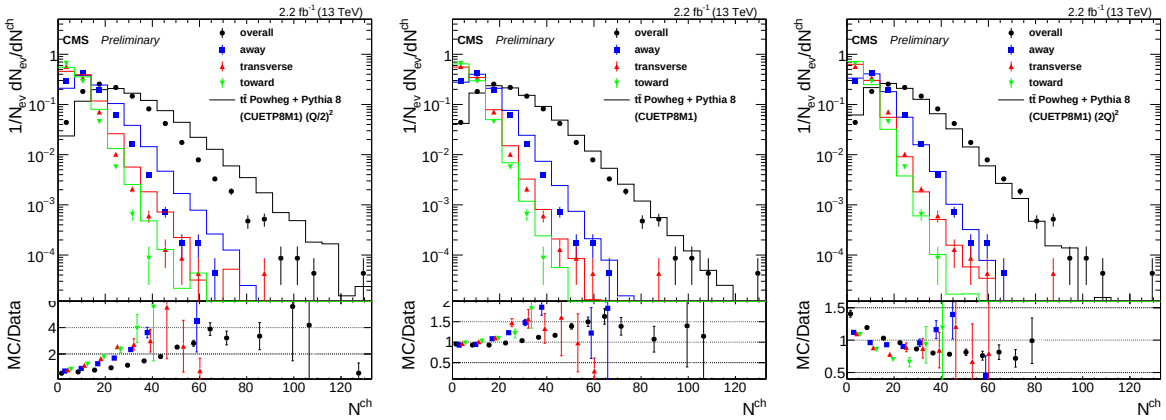

Figure 2: The charged PF candidate multiplicity distributions for the away, transverse and toward regions as well as for the overall sample. Distributions are obtained with the nominal Q^2 scale (middle) as well as $(Q/2)^2$ (left), and $(2Q)^2$ (right). The points correspond to the data at the detector level and the lines represent the POWHEG + PYTHIA 8 predictions with the CUETP8M1 tune. In this figure each distribution is normalized to one.

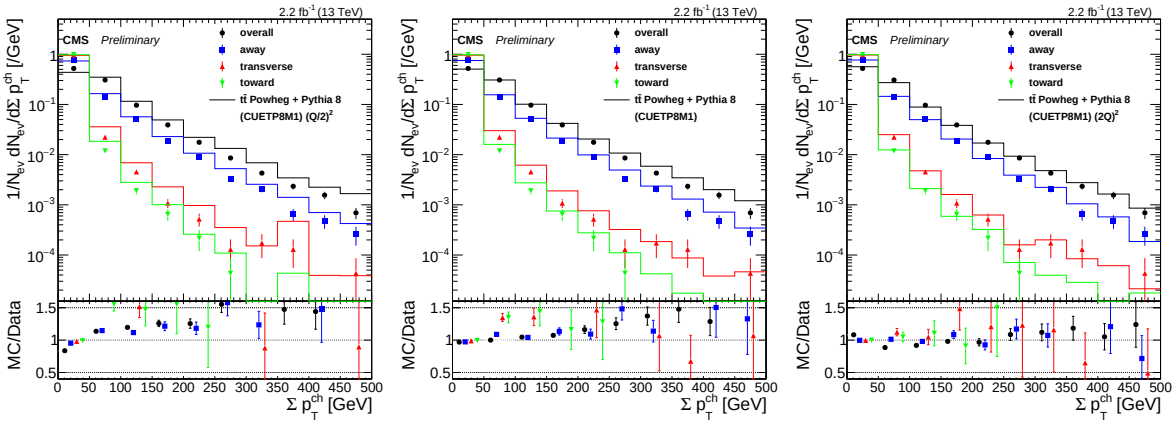

Figure 3: The transverse momentum sum distributions of the charged PF candidates for the away, transverse and toward regions as well as for the overall sample. Distributions are obtained with the nominal Q^2 scale (middle) as well as $(Q/2)^2$ (left), and $(2Q)^2$ (right). The points correspond to the data at the detector level and the lines represent the POWHEG + PYTHIA 8 predictions with the CUETP8M1 tune. In this figure each distribution is normalized to one.

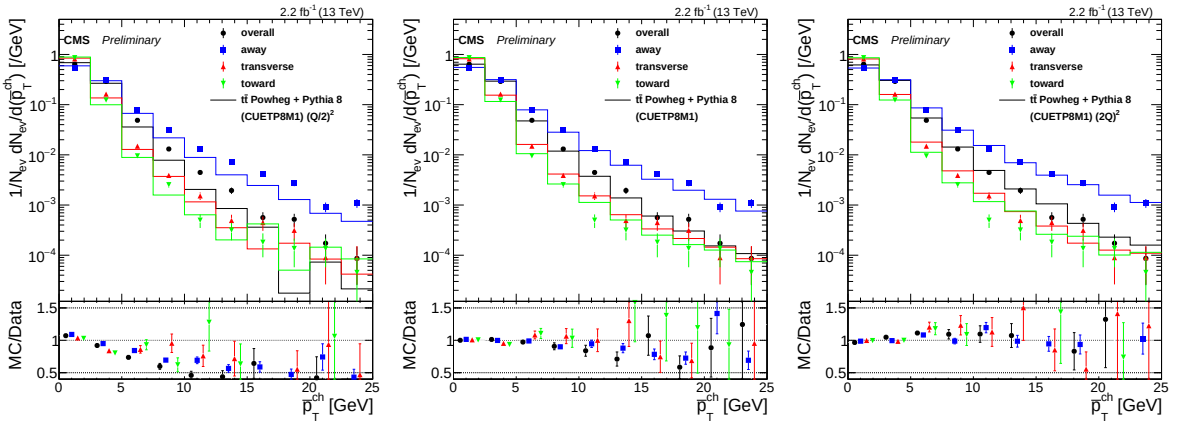

Figure 4: The average transverse momentum distributions of the charged PF candidates for the away, transverse and toward regions as well as for the overall sample. Distributions are obtained with the nominal Q^2 scale (middle) as well as $(Q/2)^2$ (left), and $(2Q)^2$ (right). The points correspond to the data at the detector level and the lines represent the POWHEG + PYTHIA 8 predictions with the CUETP8M1 tune. In this figure each distribution is normalized to one.

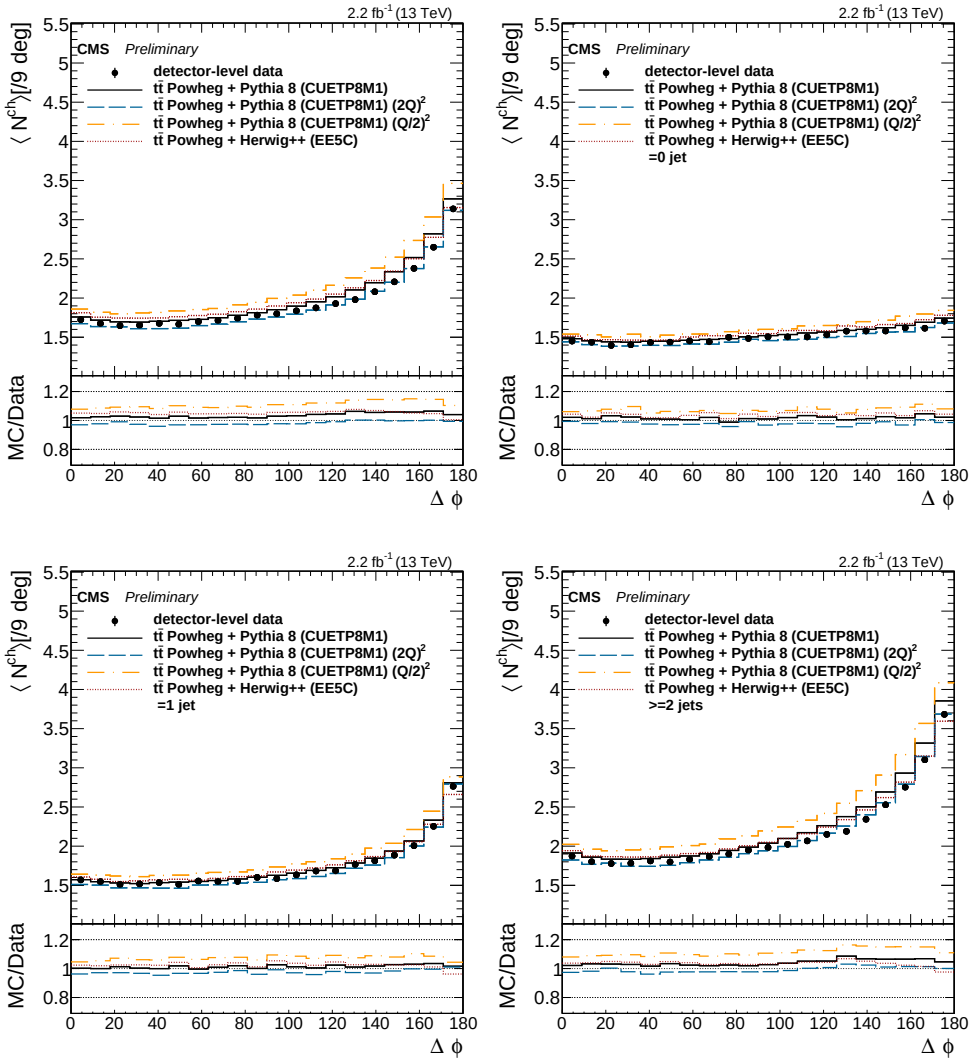

Figure 5: The number of charged particles vs the angle with respect to the event-by-event axis defined using $p_T^{t\bar{t}}$ for the inclusive and no extra jet events (top), and for the events with one and at least two extra jets (bottom). Data at the detector level are compared with the POWHEG + PYTHIA 8 predictions with the CUETP8M1 tune generated with the nominal Q^2 scale as well as $(2Q)^2$, and $(Q/2)^2$, and with the POWHEG + HERWIG ++ sample with the EE5C tune.

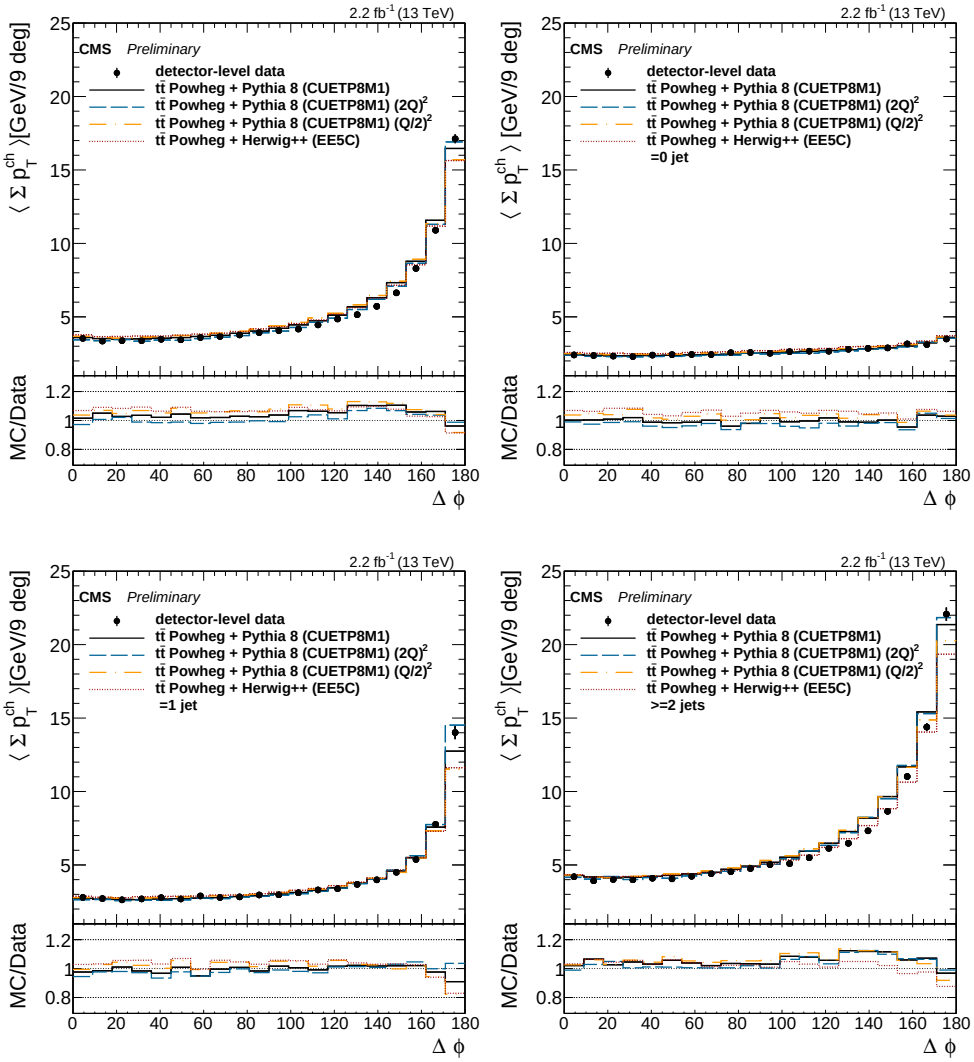

Figure 6: Sum of the charged p_T vs the angle with respect to the event-by-event axis defined using $p_T^{t\bar{t}}$ for the inclusive and no extra jet events (top), and for the events with one and at least two extra jets (bottom). Data at the detector level are compared with the POWHEG + PYTHIA 8 predictions with the CUETP8M1 tune generated with the nominal Q^2 scale as well as $(2Q)^2$, and $(Q/2)^2$, and with the POWHEG + HERWIG ++ sample with the EE5C tune.

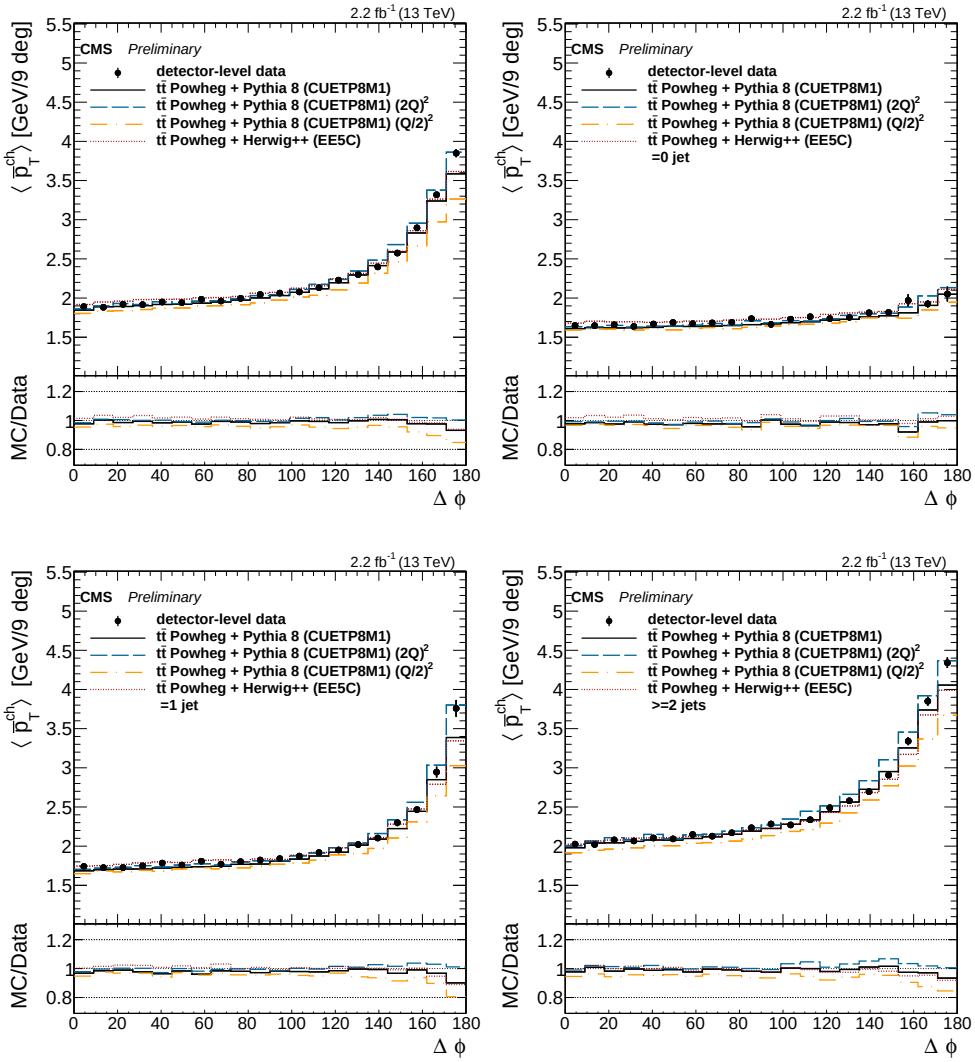

Figure 7: The average p_T per charged particle vs the angle with respect to the event-by-event axis defined using $p_T^{t\bar{t}}$ for the inclusive and no extra jet events (top), and for the events with one and at least two extra jets (bottom). Data at the detector level are compared with the POWHEG + PYTHIA 8 predictions with the CUETP8M1 tune generated with the nominal Q^2 scale as well as $(2Q)^2$, and $(Q/2)^2$, and with the POWHEG + HERWIG ++ sample with the EE5C tune.

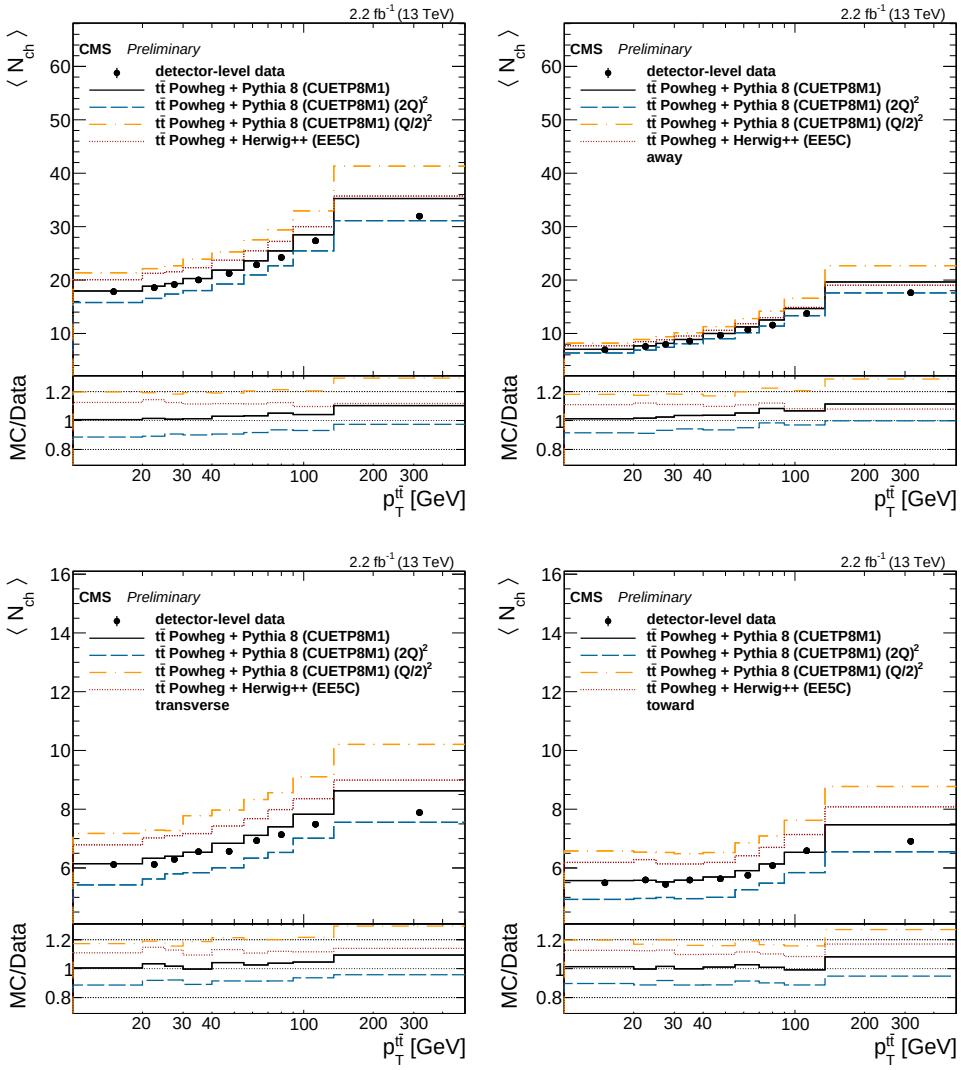

Figure 8: The number of charged particles vs $p_T^{t\bar{t}}$ for the overall sample and the away (top), transverse and toward regions (bottom) defined with respect to $\Delta\phi$. Data at the detector level are compared with the POWHEG + PYTHIA 8 predictions with the CUETP8M1 tune generated with the nominal Q^2 scale as well as $(2Q)^2$, and $(Q/2)^2$, and with the POWHEG + HERWIG ++ sample with the EE5C tune.

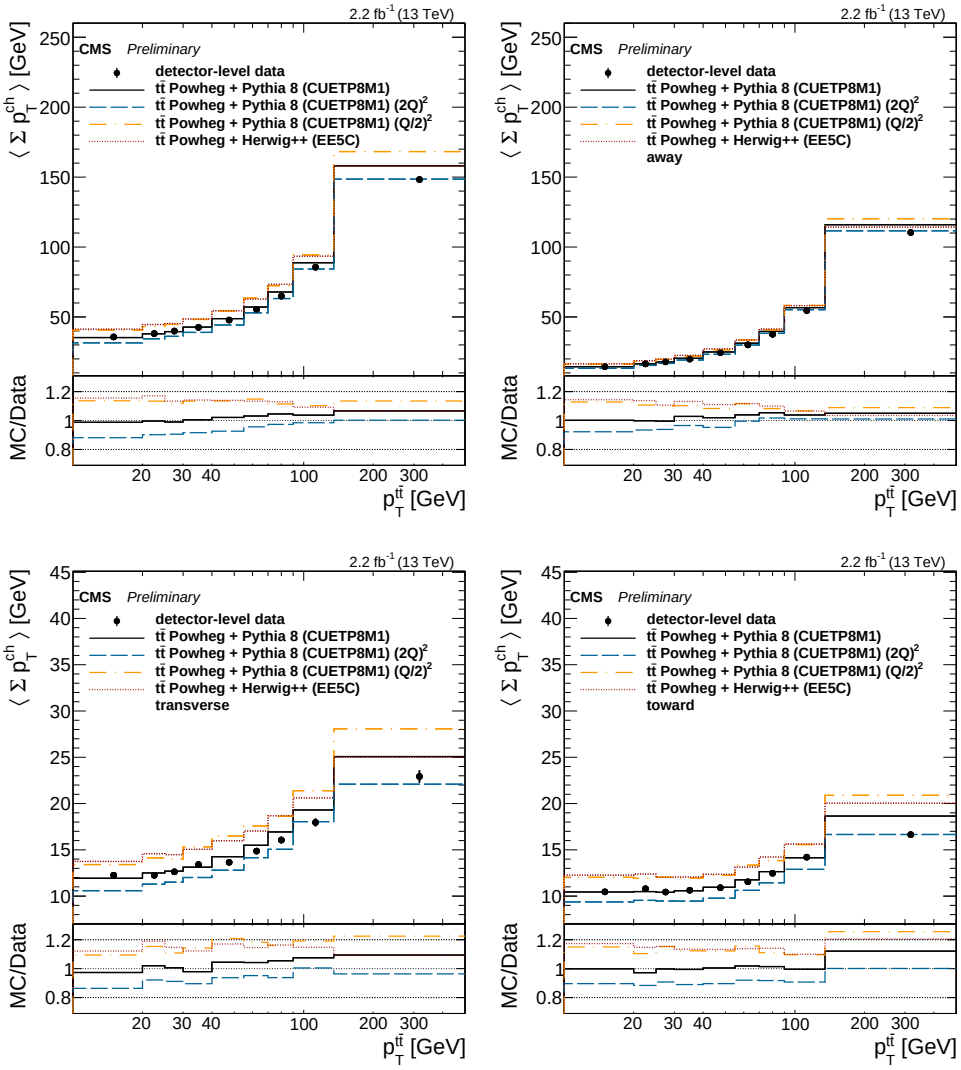

Figure 9: Sum of charged p_T vs $p_T^{t\bar{t}}$ for the overall sample and the away (top), transverse and toward regions (bottom) defined with respect to $\Delta\phi$. Data at the detector level are compared with the POWHEG + PYTHIA 8 predictions with the CUETP8M1 tune generated with the nominal Q^2 scale as well as $(2Q)^2$, and $(Q/2)^2$, and with the POWHEG + HERWIG ++ sample with the EE5C tune.

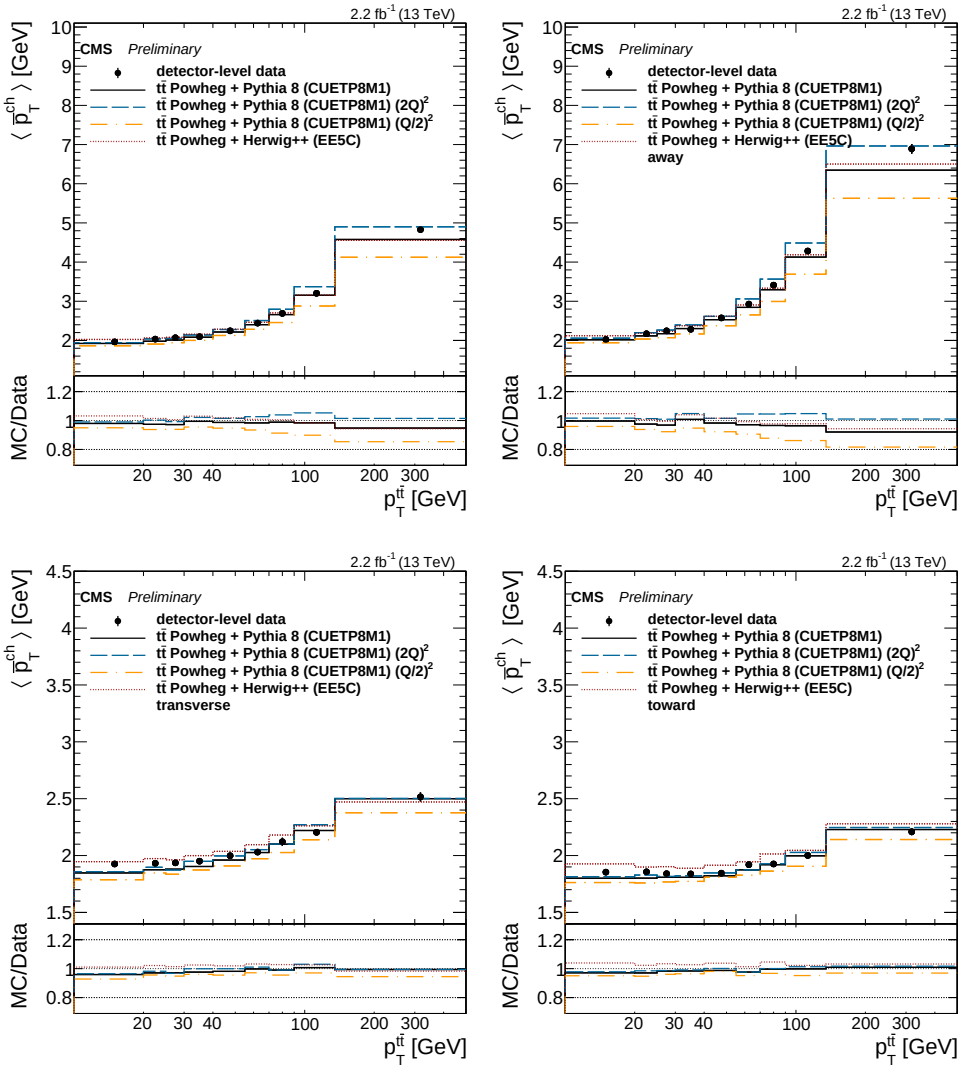

Figure 10: The average p_T per charged particle vs $p_T^{t\bar{t}}$ for the overall sample and the away (top), transverse and toward regions (bottom) defined with respect to $\Delta\phi$. Data at the detector level are compared with the POWHEG + PYTHIA 8 predictions with the CUETP8M1 tune generated with the nominal Q^2 scale as well as $(2Q)^2$, and $(Q/2)^2$, and with the POWHEG + HERWIG ++ sample with the EE5C tune.

5 Conclusions

Measurements of the underlying event (UE) activity using charged particle properties in $t\bar{t}$ events are presented. We have compared detector-level data on top-quark production at 13 TeV with the PYTHIA 8 UE tune CUETP8M1 and the HERWIG ++ UE tune EE5C after detector simulation. Both these MC models have been interfaced with the POWHEG higher order matrix element generator. When interfaced with POWHEG, both the PYTHIA 8 tune CUETP8M1 and the HERWIG ++ UE tune EE5C describe the data well, including the UE-sensitive observables. Hence, it does not appear necessary to have separate heavy-quark UE tunes.

References

[1] CMS Collaboration, "First Measurement of the Underlying Event Activity at the LHC with $\sqrt{s} = 0.9$ TeV", *Eur. Phys. J.* **C70** (2010) 555–572, doi:10.1140/epjc/s10052-010-1453-9, arXiv:1006.2083.

[2] CMS Collaboration, "Strange Particle Production in pp Collisions at $\sqrt{s} = 0.9$ and 7 TeV", *JHEP* **05** (2011) 064, doi:10.1007/JHEP05(2011)064, arXiv:1102.4282.

[3] CMS Collaboration, "Measurement of the underlying event activity in pp collisions at $\sqrt{s} = 0.9$ and 7 TeV with the novel jet-area/median approach", *JHEP* **08** (2012) 130, doi:10.1007/JHEP08(2012)130, arXiv:1207.2392.

[4] CMS Collaboration, "Jet and underlying event properties as a function of charged-particle multiplicity in protonproton collisions at $\sqrt{s} = 7$ TeV", *Eur. Phys. J.* **C73** (2013), no. 12, 2674, doi:10.1140/epjc/s10052-013-2674-5, arXiv:1310.4554.

[5] CMS Collaboration, "Study of the underlying event at forward rapidity in pp collisions at $\sqrt{s} = 0.9$, 2.76, and 7 TeV", *JHEP* **04** (2013) 072, doi:10.1007/JHEP04(2013)072, arXiv:1302.2394.

[6] CMS Collaboration, "Study of the inclusive production of charged pions, kaons, and protons in pp collisions at $\sqrt{s} = 0.9$, 2.76, and 7 TeV", *Eur.Phys.J.C* **72** (2012) 2164, doi:10.1140/epjc/s10052-012-2164-1, arXiv:1207.4724.

[7] CMS Collaboration, "Study of the underlying event, b-quark fragmentation and hadronization properties in $t\bar{t}$ events", CMS Physics Analysis Summary CMS-PAS-TOP-13-007, 2013.

[8] T. Sjostrand, S. Mrenna, and P. Skands, "A Brief Introduction to PYTHIA 8.1", *Comput. Phys. Commun.* **178** (2008) 852, doi:10.1016/j.cpc.2008.01.036, arXiv:0710.3820.

[9] M. Bahr et al., "Herwig++ Physics and Manual", *Eur.Phys.J.C* **58** (2008) 639, doi:10.1140/epjc/s10052-008-0798-9, arXiv:0803.0883.

[10] CMS Collaboration, "Event generator tunes obtained from underlying event and multiparton scattering measurements", arXiv:1512.00815.

[11] M. H. Seymour and A. Siodmok, "Constraining MPI models using σ_{eff} and recent Tevatron and LHC Underlying Event data", *JHEP* **10** (2013) 113, doi:10.1007/JHEP10(2013)113, arXiv:1307.5015.

[12] CMS Collaboration, "The CMS experiment at the CERN LHC", *JINST* **3** (2008) S08004, doi:10.1088/1748-0221/3/08/S08004.

[13] P. Nason, "A New method for combining NLO QCD with shower Monte Carlo algorithms", *JHEP* **11** (2004) 040, doi:10.1088/1126-6708/2004/11/040, arXiv:0409146.

[14] S. Frixione, P. Nason, and C. Oleari, "Matching NLO QCD computations with Parton Shower simulations: the POWHEG method", *JHEP* **11** (2007) 070, doi:10.1088/1126-6708/2007/11/070, arXiv:0709.2092.

[15] S. Alioli, P. Nason, C. Oleari, and E. Re, "A general framework for implementing NLO calculations in shower Monte Carlo programs: the POWHEG BOX ", *JHEP* **06** (2010) 043, doi:10.1007/JHEP06(2010)043, arXiv:1002.2581.

[16] J. Alwall, R. Frederix, S. Frixione et al., "The automated computation of tree-level and next-to-leading order differential cross sections, and their matching to parton shower simulations", *JHEP* **07** (2014) 079, doi:10.1007/JHEP07(2014)079, arXiv:1405.0301.

[17] R. D. Ball et al., "Parton distributions for the LHC Run II", *JHEP* **04** (2015) 040, doi:10.1007/JHEP04(2015)040, arXiv:1410.8849.

[18] S. Agostinelli et al., "Geant4: a simulation toolkit", *Nuclear Instruments and Methods in Physics Research Section A: Accelerators, Spectrometers, Detectors and Associated Equipment* **506** (2003), no. 3, 250 – 303, doi:http://dx.doi.org/10.1016/S0168-9002(03)01368-8.

[19] CMS Collaboration, "Performance of CMS muon reconstruction in pp collision events at $\sqrt{s} = 7$ TeV", *JINST* **7** (2012) P10002, doi:10.1088/1748-0221/7/10/P10002, arXiv:1206.4071.

[20] CMS Collaboration, "Determination of jet energy calibration and transverse momentum resolution in CMS", *JINST* **6** (2011) P11002, doi:10.1088/1748-0221/6/11/P11002, arXiv:1107.4277.

[21] CMS Collaboration, "b-Jet indetification in the CMS Experiment", CMS Physics Analysis Summary CMS-PAS-BTV-11-004, 2011.